Journal of Applied Polymer Science

Percolation and catalysis effect of bamboo-based active carbon on the thermal and flame retardancy properties of ethylene vinyl-acetate rubber

Hui Peng,[1] Jie Feng,[2] You Zhou,[1] Zhuoshi Li,[3] Hongfei Zou,[3] Jianwei Hao[1,3]

[1]National Engineering Research Center of Flame Retardant Materials, Beijing Institute of Technology, Beijing, China
[2]Dipartimento di Scienza Applicata e Tecnologia, Politecnico di Torino, V.le Teresa, Michel 5, 15121 Alessandria, Italy
[3]JiangSu Key laboratory of Special Cable Material and Reliability Research, Baosheng Science and Technology Innovation Co., Yangzhou, China
Correspondence to: J. Hao (E-mail: hjw@bit.edu.cn)

ABSTRACT: The effect of percolation and catalysis of bamboo-based active carbon (BAC) on the thermal degradation and flame retardancy of ethylene vinyl-acetate rubber (EVM) composites with intumescent flame retardants (IFR) consisting of ammonium polyphosphate (APP) and dipentaerythritol (DPER) has been investigated. The vulcanization characteristics were analyzed by a moving die rheometer. Thermogravimetric analysis (TGA) and fire behavior tests such as limiting oxygen index (LOI), vertical burning (UL 94), and cone calorimetry were used to evaluate the thermal properties and flame retardancy of EVM composites. Scanning electron microscopy (SEM) was used to study the morphology of residues of EVM composites. The addition of BAC significantly increased the maximum torque (M_H) of EVM composites and EVM matrices. The combination of IFR with BAC can improve the thermal stability of EVM composites. Moreover, BAC can enhance char residue and promote the formation of a network for IFR. The current EVM/37IFR/3BAC composite achieved an LOI of 33.6% and a UL 94 V-0 rating. The PHRR, total heat release (THR), and total smoke release (TSR) for EVM/IFR/BAC were greatly reduced as compared to EVM/40IFR. Also, the mechanical properties of the EVMIFR/BAC composites increased with increasing BAC contents. The physical percolation effect between BAC and EVM before and after thermal degradation, and the chemical catalysis effect between BAC and IFR during thermal degradation are responsible for the improved flame retardancy of EVM composites. © 2015 Wiley Periodicals, Inc. J. Appl. Polym. Sci. **2015**, *132*, 42414.

KEYWORDS: elastomers; flame retardance; thermogravimetric analysis

Received 2 February 2015; accepted 24 April 2015
DOI: 10.1002/app.42414

INTRODUCTION

Ethylene vinyl-acetate copolymer rubber (EVM) is a copolymer of ethylene with a high vinyl acetate content (40–80%) and is widely used for electrical insulation due to its good mechanical and physical properties.[1–4] However, the inherent flammability of EVM limits its application in some fields such as electronic appliances where high flame retardancy is required.[5–8] Hence, flame retardant additives are usually added to improve the flame retardancy of EVM.

In recent years, intumescent flame retardant (IFR) additives have been investigated by many researchers, and they have presented good flame retardance, low smoke, and excellent char-forming ability in many polymeric materials. During combustion, the intumescent system forms an expanding char layer as a barrier between the flame zone and the underlying polymeric material which improves the flame retardancy of the polymeric material. Recently, research and development have been directed towards other synergistic agents, such as clays,[9–11] metal oxides,[12] polyhedral oligomeric silsesquioxane (POSS)[13,14] and others, that may form a compact char layer to enhance the flame retardance of IFR systems. Carbon additives such as graphene,[15–17] carbon nanotubes (CNTs),[18–20] and buckminsterfullerenes[21] have been extensively explored because of their ability to increase both the mechanical strength and the flame retardant properties. It has been reported that CNTs can greatly improve electrical and rheological properties because of the formation of a percolation path.[22] A percolation path in a polymer matrix can inhibit the vigorous bubbling that occurs during combustion, and thus the use of the carbon-based fillers can reduce the flammability of polymeric materials.

Another carbon-based material is active carbons (ACs), which are amorphous carbonaceous materials with a high degree of porosity and a well-developed internal surface. ACs are usually

utilized for adsorption in gas and liquid phases,[23,24] such as purifying air from pollutants in houses and public facilities, water treatment, and so on. Moreover, ACs have been gaining in popularity as catalysts or supports for catalysts[25–27] providing potential synergism in the field of flame retardant. As compared with graphene, CNTs, and other carbon additives, ACs have many advantages such as low cost and easy preparation.

In this work, bamboo-based active carbon (BAC) was prepared via a chemical activation process with Potassium hydroxide (KOH) and an IFR system containing ammonium polyphosphate (APP), dipentaerythritol (DPER), and BAC was used to modify EVM. The percolation effect of BAC on the vulcanization characteristics of EVM composites was evaluated. Additionally, the thermal properties of ternary EVM/IFR/BAC and binary EVM/BAC and IFR/BAC and the flammability of EVM composites were also investigated.

EXPERIMENTAL

Materials

EVM700 (Levapren 700) containing 70±1.5% vinyl acetate was obtained from Lanxess Company, Germany. The commercial flame retardant additive APP was purchased from Hangzhou JLS Co., China and DPER was supplied by Jiangsu Ruiyang Chemical Co., China. The curing agent dicumyl peroxide (DCP) was provided by China Medicine (group) Chemical Reagent Center, China. The processing agents zinc oxide (ZnO) and stearic acid (SA) were supplied by Jinchuan Co., China. Bamboo piece was obtained from the bamboo forest of southeastern China. Potassium hydroxide (KOH) was purchased from Tianjing Guangfu Fine Chemical Research Institute, China. BAC was prepared in our laboratory.

Preparation of Active Carbon

The bamboo pieces were heated (10°C/min) from room temperature to 400°C and were held at this temperature for 120 min under N_2 atmosphere in a tube furnace. The products were well mixed by stirring with a concentrated solution of KOH as activating agent (the mass ratio of bamboo piece and KOH was 1 : 4) for 120 min, then the resulting homogeneous slurry was dried at 120°C for about 24 h. The resulting chemical loaded samples were heated (10°C/min) to the final carbonization temperature (700°C) and were held at this temperature for 120 min under N_2 atmosphere. The pyrolyzed samples were washed repeatedly with 0.1 mol/L solution of HCl and distilled water until free of potassium ions. Once the activating agent was removed the activated carbon sample was dried at 120°C for 12h.

Preparation of the Composites

EVM and flame retardant EVM samples were prepared at room temperature with the use of a double roller plasticator according to the formulations presented in Table I. Then, the compositions were vulcanized at 160°C under 10 MPa pressure for the optimum cure time (t_{90}, determined by a moving die rheometer).

Characterization

The cure curves of the composites were recorded in a moving die rheometer (RPA2000 TaiWan Gotech China) at 160°C. The relative curing degree was represented by the variation between the maximal torque value (M_H) and the minimal torque value (M_L) of the curing curve.

Table I. Formulations of the EVM Composites

Sample[a]	EVM (wt %)	IFR[b] (wt %)	BAC (wt %)
EVM	100	0	0
EVM/40IFR	60	40	0
EVM/39IFR/1BAC	60	39	1
EVM/38IFR/2BAC	60	38	2
EVM/37IFR/3BAC	60	37	3
EVM/36IFR/4BAC	60	36	4
EVM/3BAC	97	0	3
EVM/25IFR	75	25	0
EVM/23.1IFR/1.9BAC	75	23.1	1.9

[a] The addition of other additives DCP, ZnO, and SA was about 1∼2 wt %, respectively.
[b] IFR consisting of APP/ DPER (mass ratio of 3 : 1).

Thermogravimetric analysis (TGA) was performed using a Netzsch TG 209 F1 apparatus to investigate the thermal degradation of the flame retardant EVM system under N_2 atmosphere. The samples (2.5±0.2mg) were heated in an alumina crucible from 50°C to 800°C at a heating ramp of 20°C·min^{-1}. The calculated thermogravimetric (TG) and derivative thermogravimetric (DTG) curves were obtained according to the following equation.

$$W_{cal}(T) = x_i W_i(T)$$

where x_i is the content of compound i and W_i is TG or DTG curve of compound i.

LOI was measured on an FTA-II instrument (Rheometric Scientific) with the specimen dimensions of 130×6.5×3 mm^3, according to ASTM D 2863-2008. The vertical burning test was carried out with a CZF-3 instrument (Jiangning Analysis Instrument Factory) with a specimen dimension of 125×12.5×3.2 mm^3, according to ASTM D 3801-2010.

The combustion test was performed on the cone calorimeter (FTT, United Kingdom). All samples (100×100×3 mm^3) were wrapped in an aluminum foil and exposed horizontally to an external heat flux of 35 kW/m^2. The cone data reported here was an average of three replicated measurements.

Scanning electron microscopy (SEM) analysis of the prepared BAC and char residues were observed on a ZEISS Supra-55 microscopy. All the specimens were previously coated with a conductive gold.

The mechanical properties were measured with a universal testing machine (Instron 1185) at temperatures 25±2°C. The crosshead speed was 200 mm/min. Dumbbell-shaped specimens were prepared according to ASTM D 412–2006. The tensile strength and elongation at break were recorded.

RESULTS AND DISCUSSION

Percolation Effect

Recently, many researchers found that the percolation threshold of polymer composites based on CNTs was connected to its

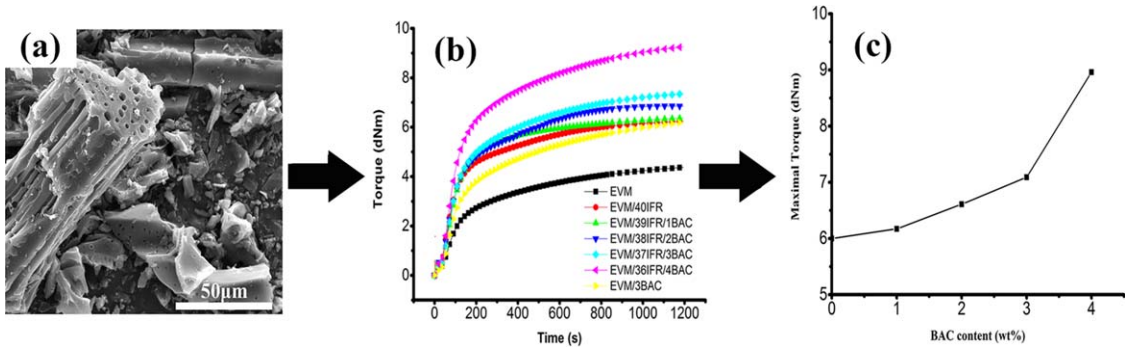

Figure 1. The percolation effect of BAC in EVM composites. (a) SEM micrograph of BAC; (b) The curing curves of EVM composites; (c) Effect of BAC content on the maximum torque of EVM/IFR/BAC composites. [Color figure can be viewed in the online issue, which is available at wileyonlinelibrary.com.]

microstructure, such as its aspect ratio, specific area, and so on.[28] To evaluate the potential percolation effect of BAC in EVM composites, an SEM micrograph of BAC, the curing curves of EVM composites at 160°C, and the effect of BAC content on the maximum torque (M_H) of EVM/IFR/BAC composites are shown in Figure 1, the rheometric characteristics are listed in Table II. From the SEM micrograph of BAC in Figure 1(a), many well-developed pores with diameters of 2∼5 μm were clearly found on the surface of the BAC. This special pore structure could facilitate the percolation effect of BAC in EVM composites. As seen from Figure 1(b) and Table II, the minimum torque (M_L) and the scorch time (t_{10}) were nearly invariable, indicating the addition of IFR and BAC did not affect the processability and scorch safety of the EVM composites. Interestingly, M_H and the optimum time (t_{90}) not only increased with increasing BAC content in the EVM composites, they also obviously increased by adding BAC alone in the EVM matrix. The increase of M_H is associated with the increasing crosslink density, which can probably be ascribed to the percolation effect of BAC resulting in the formation of an entangled and mechanically rigid network [Figure 1(c)]. The increased crosslink density means higher melt viscosity which can decrease the growth rate of volatile degradation products.[29] It should also benefit char formation during the thermal degradation of EVM composites. Here, BAC showed a good performance in terms of high crosslink density, but the relation between the microstructure and the percolation threshold of BAC should be studied further.

Table II. Rheometric Characteristics of EVM Composites at 160°C

Sample	M_L (dNm)	t_{10} (s)	M_H (dNm)	T_{90} (min : s)
EVM	0.19	51	4.27	12 : 12
EVM/40IFR	0.21	45	6.00	7 : 47
EVM/39IFR/1BAC	0.20	50	6.17	9 : 02
EVM/38IFR/2BAC	0.20	49	6.61	9 : 31
EVM/37IFR/3BAC	0.15	50	7.09	10 : 29
EVM/36IFR/4BAC	0.20	49	8.96	11 : 10
EVM/3BAC	0.10	51	6.06	12 : 27

Thermal Degradation and Charring Behavior

The influence of BAC on the thermal behavior of EVM/IFR, IFR, and EVM was investigated by TGA. From the results in Figures 2 and 3, and Table III, EVM under N_2 atmosphere

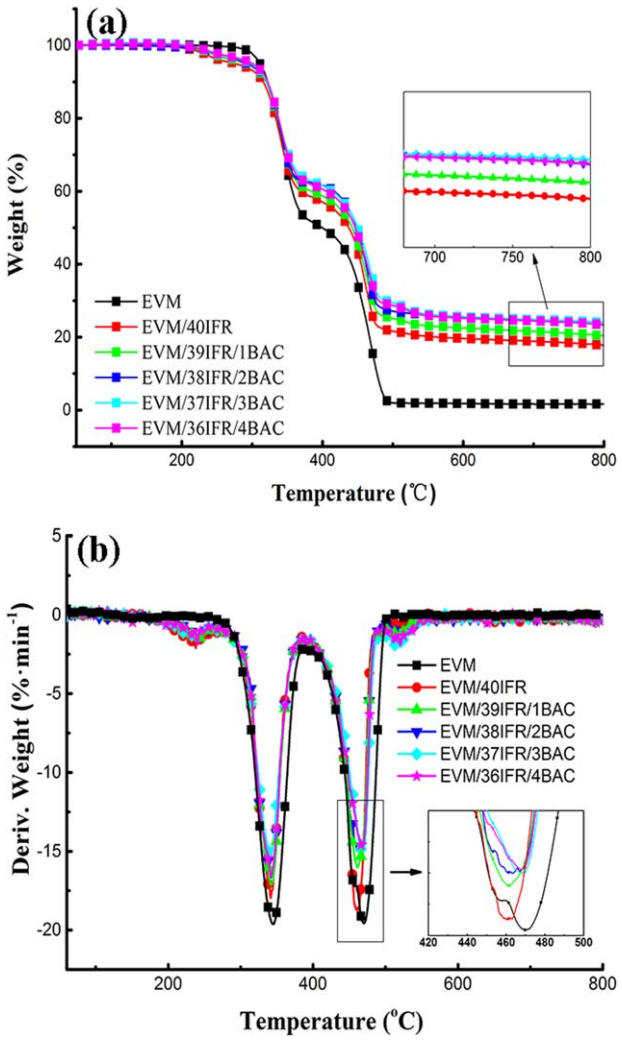

Figure 2. (a) TG and (b) DTG curves of EVM composites in N_2. [Color figure can be viewed in the online issue, which is available at wileyonlinelibrary.com.]

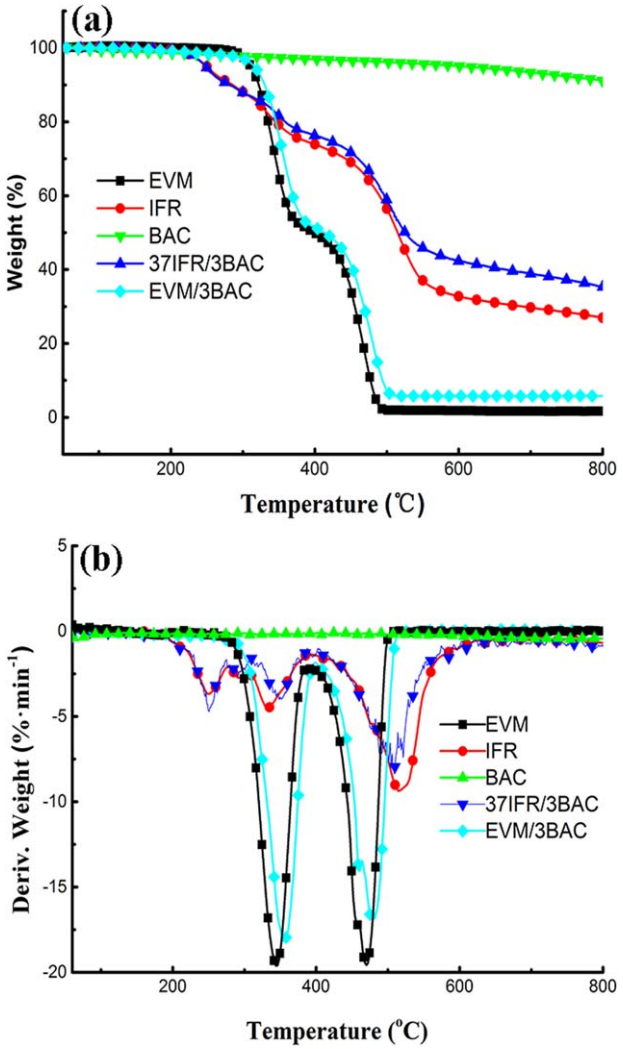

Figure 3. (a) TG and (b) DTG curves of EVM/BAC (mass ratio of 37 : 3) and IFR/BAC (mass ratio of 97 : 3) in N_2. [Color figure can be viewed in the online issue, which is available at wileyonlinelibrary.com.]

showed two decomposition steps with a maximum mass loss rate (R_{max}) and minimum char residues of 1.6 wt % ($CR_{800°C}$) at 800°C. The first stage of thermal decomposition was related to the elimination of acetic acid and the formation of unsaturated polyenes, whereas the second stage was related to the completely degradation of these polyenes.[30,31] The addition of IFR decreased the initial thermal decomposition temperature ($T_{5\%}$, based on 5% mass loss) from 311 to 276°C, but it also significantly enhanced the char residue at 800°C as compared to pure EVM. It is worth noting that with increasing BAC loading, $T_{5\%}$ of the EVM/IFR/BAC composites increased and it was higher than that of EVM/40IFR. At the same time, the maximum mass loss rate at the second stage (R_{2max}) decreased, and its related temperature (T_{2max}) and the char residue ($CR_{800°C}$) at 800°C tended to increase with increasing BAC content. Especially, the experimental char residue of EVM/37IFR/3BAC reached 24.1 wt %, which is much higher than that of EVM/40IFR and the calculated value (13.7 wt %). This clearly indicates that the percolation effect of BAC built up a particle network which resulted in improving the thermal stability in the first stage of decomposition. Also, the particle network provided a physical barrier for the transfer of heat and mass, thus delaying the random scission of polymer chains and increasing the amount of char residue in the second stage at high temperatures. Similar results were also observed for the polypropylene (PP) nanocomposites filled with functionalized graphene.[32]

The interaction between BAC and EVM or BAC and IFR was also investigated by TGA. As shown in Figure 3 and Table III, when adding BAC to EVM, the $T_{5\%}$, T_{1max}, T_{2max}, and $CR_{800°C}$ of EVM increased, which is related to the percolation effect of BAC. It is obvious that R_{1max} and R_{2max} also decreased because the physical barrier effect of the network-like structure of BAC slowed the decomposition of the EVM matrix. Similar results were found with EVM/IFR/BAC composites. IFR decomposed in three steps, and its char residue at 800°C was 26.9 wt %; BAC remained nearly a constant weight and its char residue at 800°C was 93.0 wt %. When BAC was introduced into IFR, its

Table III. Thermal Analysis Data under Pure N_2 by TGA

		First stage		Second stage		Third stage		$CR_{800°C}$[a] (%)	
Sample	$T_{5\%}$ (°C)	R_{1max} (%·min^{-1})	T_{1max} (°C)	R_{2max} (%·min^{-1})	T_{2max} (°C)	R_{3max} (%·min^{-1})	T_{3max} (°C)	Exp.	Cal.
EVM	311	19.6	343	19.6	469	-	-	1.6	-
EVM/40IFR	276	18.0	341	18.7	463	-	-	17.8	11.7
EVM/39IFR/1BAC	291	17.1	341	16.0	462	-	-	20.4	12.4
EVM/38IFR/2BAC	292	16.3	342	15.0	463	-	-	23.3	13.1
EVM/37IFR/3BAC	298	15.3	341	15.0	468	-	-	24.1	13.7
EVM/36IFR/4BAC	300	16.6	341	14.7	467	-	-	23.4	14.4
IFR	250	3.5	252	4.4	332	9.2	519	26.9	-
BAC	-	-	-	-	-	-	-	93.0	-
37IFR3/BAC	247	4.2	252	3.7	353	7.4	507	35.3	31.9
EVM/3BAC	316	18.2	354	16.9	481	-	-	5.8	5.2

[a] $CR_{800°C}$ is the experimental (Exp.) value and the calculated (Cal.) value of char residue at 800°C under pure N_2.

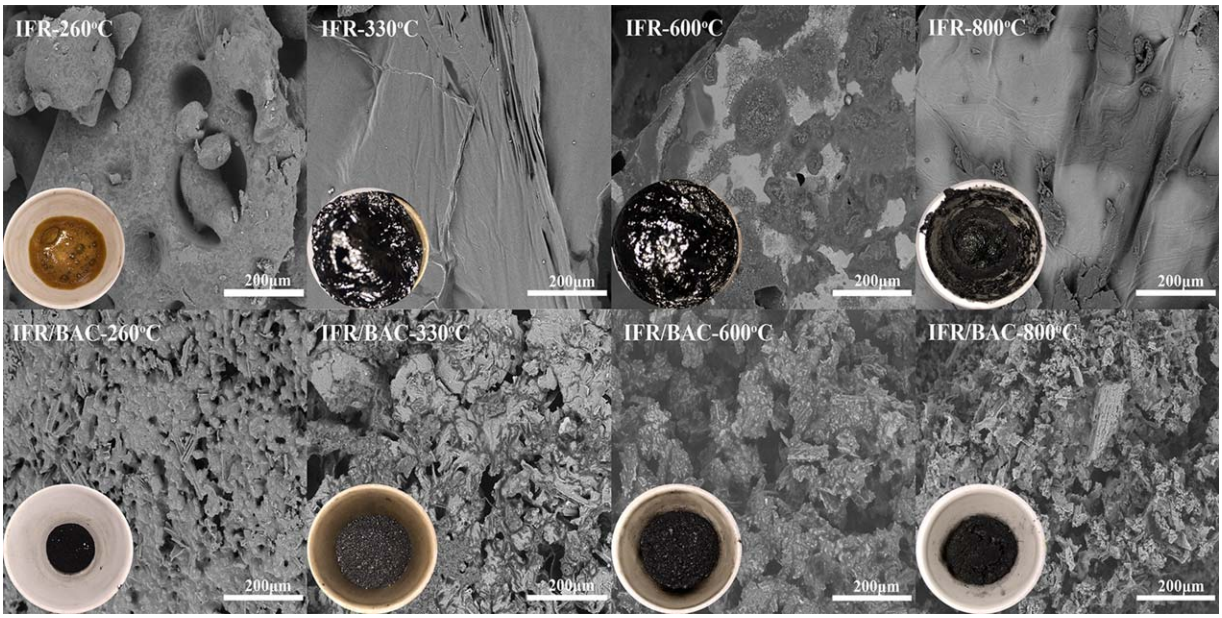

Figure 4. SME micrographs and digital photos of IFR and IFR/BAC (mass ratio of 37 : 3) at different decomposition temperature. [Color figure can be viewed in the online issue, which is available at wileyonlinelibrary.com.]

$T_{5\%}$ shifted to a slightly lower temperature; R_{1max} increased to 4.2%/min in the first stage, and R_{3max} in the third stage was 7.4%/min, which was lower than that for IFR (9.2%/min). These phenomena demonstrated that BAC could catalyze the release of H_2O and NH_3 of IFR at the initial stage, and reduce the volatilization of decomposition products (such as P_2O_5) at the higher-temperature stage.[33,34] As a result, more residues (35.3 wt %) were obtained than the calculated amount (31.9 wt %) in the condensed phase. In conclusion, the percolation effect of BAC improved the thermal stability of EVM composites and the catalysis effect of BAC favored more char residue for IFR.

Residues and Char Morphology

To further understand the catalysis and char formation effect of BAC on IFR, Figure 4 shows the SEM micrographs and digital photos of the outer layer of IFR and IFR/BAC (mass ratio of 37 : 3) at different decomposition temperatures. According to the digital photos in Figure 4, IFR began to melt and bubble at 260°C. As the temperature increased to 330°C, intumescent char was found for IFR, and it remained unchanged at 600°C. At 800°C, this intumescent char fractured and left a small amount of residue. Compared to IFR, IFR/BAC formed a compact residue because the expansion of the char residue of IFR was restrained by the BAC network at lower temperatures. Also, the char morphology retained a compact structure with increasing temperature. From the SEM micrographs in Figure 4, char residue with large cell can be found for IFR, whereas many closed small cells appeared in that of IFR/BAC. This phenomenon is mainly attributed to the formation of a network by the catalysis and char formation effect of BAC, which is related to the high specific surface area of BAC, and this led to the attachment of decomposition products to the surface of the BAC network.

Fire Behavior

The flame retardant properties of the EVM composites were evaluated by LOI, UL 94, and cone calorimeter. Table IV summarizes the test results for all samples. With pure EVM, the LOI value of 23.2% indicates its flammable nature. The LOI value of EVM/40IFR was 31.7%. When 1.0–4.0 wt % of IFR was substituted by BAC, the LOI values were higher than that with IFR alone. An optimum was observed at 37 wt % of IFR and 3 wt % of BAC, which resulted in an LOI value of 33.6%. Also, all the IFR EVM composites reached the V-0 rating in the UL 94 test (both 3.2 mm and 1.6 mm).

Based on the ratio of 37 : 3 for IFR and BAC, the effect of the flame-retardant loading on the flame retardancy of EVM was also investigated. When the total loading of IFR and IFR/BAC in EVM was 25 wt %, the LOI values of EVM/25IFR and EVM/23.1IFR/1.9BAC were 27.0% and 28.7%, respectively. In addition, it was found that these two samples reached the V-0 rating with a thickness of 3.2 mm. When the thickness decreased to 1.6 mm, EVM/25IFR reached a V-2 rating, whereas EVM/23.1IFR/1.9BAC reached a V-1 rating. This difference suggests

Table IV. LOI and UL 94 Results of EVM Composites

			UL 94	
Sample	LOI (%)	ΔLOI (%)	3.2 (mm)	1.6 (mm)
EVM	23.2	-	N. R.	N. R.
EVM/40IFR	31.7	8.5	V-0	V-0
EVM/39IFR/1BAC	32.3	9.1	V-0	V-0
EVM/38IFR/2BAC	32.8	9.6	V-0	V-0
EVM/37IFR/3BAC	33.6	10.4	V-0	V-0
EVM/36IFR/4BAC	33.1	9.9	V-0	V-0
EVM/25IFR	27.0	3.8	V-0	V-2
EVM/23.1IFR/1.9BAC	28.7	5.5	V-0	V-1

Table V. CONE Test Results of EVM Composites (Irradiance 35 kW/m^2)

Sample	TTI (s)	PHRR (kW/m^2)	THR (MJ/m^2)	TSR (m^2/m^2)	Residue (%)	FPI
EVM	49±2	765±13	104.4±0.9	2291±35	3.7±0.5	0.064
EVM/40IFR	57±3	233±6	52.3±0.7	2122±29	21.8±1.0	0.245
EVM/39IFR/1BAC	51±4	226±7	60.4±0.7	1993±31	33.4±1.1	0.225
EVM/38IFR/2BAC	58±3	168±5	49.1±0.6	1883±33	37.1±1.2	0.346
EVM/37IFR/3BAC	54±2	167±4	42.4±0.6	1915±28	45.1±1.9	0.323
EVM/36IFR/4BAC	52±3	226±6	55.2±0.6	1878±30	38.0±0.9	0.230

that BAC had a significant effect on improving the flame retardancy of EVM/IFR composites.

Cone calorimeter is an effective bench-scale apparatus to simulate real fire scenarios.[35] The detailed combustion parameters of the EVM/IFR composites at a heat flux of 35 kW/m^2 are listed in Table V. The curves of the heat release rate (HRR) and THR are also given in Figure 5. As shown in Table V, the times to ignition (TTI) of the EVM/IFR composites were longer than that of the pure EVM. Also, in comparison to pure EVM, the peak heat release rate (PHRR) and THR of EVM/40IFR were reduced by 69.6% and 49.9%, respectively. Moreover, as compared to EVM/IFR, the PHRR and THR of EVM/IFR/BAC were further reduced. The lowest values of PHRR and THR are found in EVM/37IFR/3BAC which is in agreement with the results of the LOI test. This phenomenon can be explained as follows: the amount of char residue increased by the percolation and catalysis effect of BAC providing a protective layer to insulate heat and mass. It is also observed that BAC decreased the release of smoke from the combustion of EVM/IFR/BAC composites. This is attributed to the formation of a network-like structure due to the presence of BAC. That is to say, BAC improved the condensed phase flame retardation effect.

In order to evaluate the fire behavior of EVM/IFR composites more clearly, the fire performance index (FPI) was selected. The FPI is defined as the ratio of TTI and PHRR. There is a certain correlation between the value of FPI and the real-time to

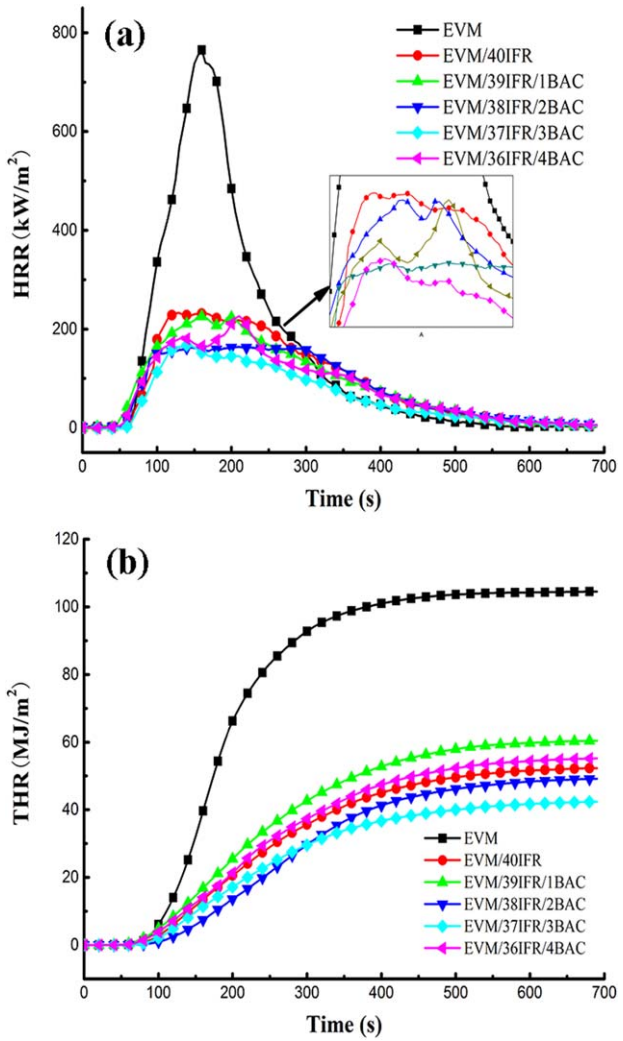

Figure 5. (a) Heat release rate and (b) total heat release of EVM composites at 35 kW/m^2. [Color figure can be viewed in the online issue, which is available at wileyonlinelibrary.com.]

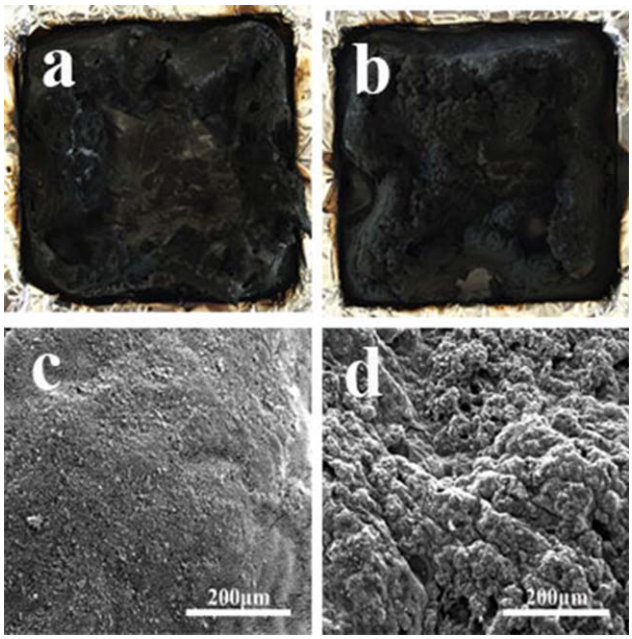

Figure 6. (a,b) Digital photos and (c,d) SME micrographs of char residues after cone test. (a,c) EVM/40IFR and (b,d) EVM/37IFR/3BAC. [Color figure can be viewed in the online issue, which is available at wileyonlinelibrary.com.]

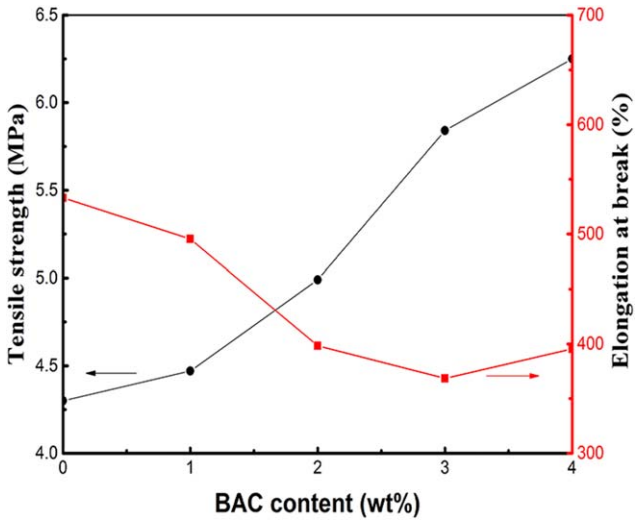

Figure 7. Effect of BAC content on the mechanical properties of EVM/IFR/BAC composites. [Color figure can be viewed in the online issue, which is available at wileyonlinelibrary.com.]

flashover. The higher the FPI, the longer the time to flashover is. Apparently, when 2 wt % or 3 wt % of BAC was added, the fire risk of the EVM composites was smaller.

The formation of a compact char is favorable to the reduction of HRR and THR, and thus it is an indication of good fire retardant effectiveness. Figure 6 shows photographs and the corresponding SEM micrographs of char residues for EVM/40IFR (a, c) and EVM/37IFR/3BAC (b, d) after the cone test. As compared to EVM/40IFR, the center of EVM/37IFR/3BAC was swollen, and more bursting bubbles on the surface with a high amount of char residue could be observed. From Figure 6, a continuous and loose carbonaceous structure is observed in the surface of the EVM/40IFR char [Figure 6(c)], whereas a compact and dense surface is observed for EVM/37IFR/3BAC char [Figure 6(d)]. This compact and dense structure can provide a better barrier and inhibit the transfer of heat when exposed to flame or a heat source. The above result is additional evidence demonstrating the percolation and catalysis effect of BAC and the synergistic effect between IFR and BAC.

Based on the results mentioned above, the improved flame retardancy of EVM composites is mainly attributed to two reasons. On one hand, the formation of a network-like structure of BAC due to its percolation effect in EVM composites increased the melt viscosity, which favors the formation of a more compact protective layer. This could be referred to as a physical effect. On the other hand, the chemical catalysis effect between IFR and BAC increased the char residue at high temperatures. It not only reduced the release of flammable degradation products, but it also formed a more effective char which inhibited the oxygen and feedback of heat reaching the underlying substrate. Therefore, both the physical and chemical effects of BAC played a role in improving the flame retardancy of EVM composites.

Mechanical Properties

Figure 7 displays the tensile strength and elongation at break of the EVM/IFR/BAC composites with various concentrations of BAC. It is clear that all the composites showed increasing tensile strength with increasing BAC loadings. This observation is the same as the tensile stress behavior of polyetherimide (PEI)/CNT composites.[36] The stress on the material transferred from the EVM molecules to the BAC network-like structure, and hence the tensile strength increased. The elongation at break decreased for EVM/IFR/BAC composites, because BAC acted as a stress concentrator within EVM. This can be considered additional evidence for the percolation effect of BAC.

CONCLUSIONS

The combination of IFR and BAC, activated carbon based on bamboo, was used to prepare EVM composites. The percolation effect based on BAC within EVM composites formed a network which increased the maximum torque. The BAC network-like structure inhibited the transfer of heat and mass between the polymer and the flame effectively during the combustion of the EVM composites. According to the TGA, the addition of BAC increased the initial thermal decomposition temperature and the char residue increased from 17.8 wt % for EVM/40IFR to 24.1 wt % for EVM/37IFR/3BAC. Meanwhile, based on the analysis of binary EVM/BAC and IFR/BAC, the percolation effect of BAC reduced the rate of EVM decomposition, whereas BAC catalyzed the release of H_2O and NH_3 and promoted the formation of char residue of IFR. Moreover, the incorporation of IFR and BAC together result a better flame retardancy and higher tensile strength for EVM than IFR alone. As a conclusion, the percolation and catalysis effect of BAC were the main reasons for the improved flame retardancy of intumescent EVM composites.

REFERENCES

1. Wang, B. B.; Wang, X. F.; Shi, Y. Q.; Tang, G.; Tang, Q. B.; Song, L.; Hu, Y. *Radiat. Phys. Chem.* **2012**, *81*, 308.
2. Rybinski, P.; Janowska, G.; Plis, A. *Therm. Acta.* **2013**, *568*, 104.
3. Li, B.; Jia, H.; Guan, L. M.; Bing, B. C.; Dai, J. F. *J. Appl. Polym. Sci.* **2009**, *114*, 3626.
4. Wang, L. C.; Wu, X. F.; Wu, C.; Yu, J. H.; Wang, G. L.; Jiang, P. K. *J. Appl. Polym. Sci.* **2011**, *121*, 68.
5. Ye, L.; Qu, B. J. *Polym. Degrad. Stab.* **2008**, *93*, 918.
6. Fernandez, A. I.; Haurie, L.; Formosa, J.; Chimenos, J. M.; Antunes, M.; Velasco, J. I. *Polym. Degrad. Stab.* **2008**, *94*, 57.
7. Basfar, A. A.; Bae, H. J. *J. Fire Sci.* **2010**, *28*, 161.
8. Wu, X. F.; Wang, L. C.; Wu, C.; Yu, J. H.; Xie, L. Y.; Wang, G. L.; Jiang, P. K. *Polym. Degrad. Stab.* **2012**, *97*, 54.
9. Zhang, R. C.; Hong, S. M.; Koo, C. M. *J. Appl. Polym. Sci.* **2014**, *131*, 40648.
10. Deng, C.; Zhao, J.; Deng, C. L.; Lv, Q.; Chen, L.; Wang, Y. Z. *Polym. Degrad. Stab.* **2014**, *103*, 1.
11. Zhu, F.; Liu, D.; Cai, G. P.; Tan, X. F.; Wang, J.; Lu, H. D.; Wilkie, C. A. *Polym. Adv. Technol.* **2014**, *25*, 211.
12. Friederich, B.; Laachachi, A.; Sonnier, R.; Ferriol, M.; Cochez, M.; Toniazzo, V.; Ruch, D. *Polym. Adv. Technol.* **2012**, *23*, 1369.

13. Pan, M.; Guan, D. B.; Wang, T. T.; Huang, R.; Mu, J. X.; Zhang, C. L. *High Perform. Polym.* **2013**, *25*, 992.
14. Xue, M.; Zhang, X.; Ma, L.; Gu, Z.; Lin, Y. X.; Bao, C.; Tian, X. Y. *J. Appl. Polym. Sci.* **2013**, *128*, 2395.
15. Wang, X.; Song, L.; Yang, H. Y.; Lu, H. D.; Hu, Y. *Ind. Eng. Chem. Res.* **2011**, *50*, 5376.
16. Liao, S. H.; Liu, P. L.; Hsiao, M. C.; Teng, C. C.; Wang, C. A.; Ger, M. D.; Chiang, C. L. *Ind. Eng. Chem. Res.* **2012**, *51*, 4573.
17. Huang, G. B.; Gao, J. R.; Wang, X.; Liang, H. D.; Ge, C. H. *Mater. Lett.* **2012**, *66*, 187.
18. Lu, K.; Cao, X. J.; Liang, Q. S.; Wang, H. T.; Cui, X. W.; Li, Y. J. *Ind. Eng. Chem. Res.* **2014**, *53*, 8784.
19. Moon, S. C.; Kim, J. Y.; Oh, B. T. *Polym. Eng. Sci.* **2014**, *54*, 1289.
20. Ebadi, M.; Mirdamadian, Z.; Ghanbari, D.; Moradi, L. *J. Clust. Sci.* **2014**, *25*, 541.
21. Song, P. A.; Liu, H.; Shen, Y.; Du, B. X.; Fang, Z. P.; Wu, Y. *J. Mater. Chem.* **2009**, *19*, 1305.
22. Liu, Y. D.; Kumar, S. *ACS Appl. Mater. Inter.* **2014**, *6*, 6069.
23. Daifullah, A. A. M.; Girgis, B. S.; Gad, H. M. H. *Mater. Lett.* **2003**, *57*, 1723.
24. Hesas, R. H.; Arami-Niya, A.; Daud, W. M. A. W.; Sahu, J. N. *Bioresources* **2013**, *8*, 2950.
25. Bonarowska, M.; Rarog-Pilecka, W.; Karpinski, Z. *Catal. Today* **2011**, *169*, 223.
26. Sakanishi, K.; Wu, Z. H.; Matsumura, A.; Saito, I.; Hanaoka, T.; Minowa, T.; Tada, M.; Iwasaki, T. *Catal. Today* **2005**, *104*, 94.
27. Alegre, C.; Galvez, M. E.; Baquedano, E.; Pastor, E.; Moliner, R.; Lazaro, M. J. *Int. J. Hydrogen Energ.* **2012**, *37*, 7180.
28. Shehzad, K.; Ahmad, M. N.; Hussain, T.; Mumtaz, M.; Shah, A. T.; Mujahid, A.; Wang, C.; Ellingsen, J.; Dang, M. Z. *J. Appl. Phys.* **2014**; *116*; 064908.
29. Ye, L.; Miao, Y. Y.; Yan, H.; Li, Z.; Zhou, Y. L.; Liu, J. X.; Liu, H. *Polym. Degrad. Stab.* **2013**, *98*, 868.
30. Cerin, O.; Duquesne, S.; Fontaine, G.; Roos, A.; Bourbigot, S. *Polym. Degrad. Stab.* **2011**, *96*, 1812.
31. Liu, H.; Xiong, Y. Q.; Xu, W. J.; Zhang, Y. J.; Pan, S. J. *J. Appl. Polym. Sci.* **2012**, *125*, 1544.
32. Dittrich, B.; Wartig, K. A.; Hofmann, D.; Mulhaupt, R.; Schartel, B. *Polym. Advan. Technol.* **2013**, *24*, 916.
33. Dahiya, J. B.; Rathi, S.; Bockhorn, H.; Kandola, B. K. *Polym. Degrad. Stab.* **2012**, *97*, 1458.
34. Gu, J. W.; Zhang, G. C.; Dong, S. L.; Zhang, Q. Y.; Kong, J. *Surf. Coat. Technol.* **2007**, *201*, 7835.
35. Feng, J.; Hao, J. W.; Du, J. X.; Yang, R. J. *Polym. Degrad. Stab.* **2012**, *97*, 605.
36. Isayev, A. I.; Kumar, R.; Lewis, T. M. *Polymer* **2009**, *50*, 250.